

Role of chemotaxis in the transport of bacteria through saturated porous media

Roseanne M. Ford ^{a,*}, Ronald W. Harvey ^b

^a Department of Chemical Engineering, University of Virginia, Charlottesville, VA 22904, United States

^b Water Resources Division, United States Geological Survey, Boulder, CO 80303, United States

Received 8 January 2006; received in revised form 16 April 2006; accepted 5 May 2006

Available online 14 September 2006

Abstract

Populations of chemotactic bacteria are able to sense and respond to chemical gradients in their surroundings and direct their migration toward increasing concentrations of chemicals that they perceive to be beneficial to their survival. It has been suggested that this phenomenon may facilitate bioremediation processes by bringing bacteria into closer proximity to the chemical contaminants that they degrade. To determine the significance of chemotaxis in these processes it is necessary to quantify the magnitude of the response and compare it to other groundwater processes that affect the fate and transport of bacteria. We present a systematic approach toward quantifying the chemotactic response of bacteria in laboratory scale experiments by starting with simple, well-defined systems and gradually increasing their complexity. Swimming properties of individual cells were assessed from trajectories recorded by a tracking microscope. These properties were used to calculate motility and chemotaxis coefficients of bacterial populations in bulk aqueous media which were compared to experimental results of diffusion studies. Then effective values of motility and chemotaxis coefficients in single pores, pore networks and packed columns were analyzed. These were used to estimate the magnitude of the chemotactic response in porous media and to compare with dispersion coefficients reported in the field. This represents a compilation of many studies over a number of years. While there are certainly limitations with this approach for ultimately quantifying motility and chemotaxis in granular aquifer media, it does provide insight into what order of magnitude responses are possible and which characteristics of the bacteria and media are expected to be important.

© 2006 Elsevier Ltd. All rights reserved.

Keywords: Bacteria; Chemotaxis; Motility; Diffusion; Dispersion; Groundwater; Bioremediation; Transport; Migration; Porous media; Pore-scale

1. Introduction

Many soil-inhabiting bacteria that degrade chemical contaminants are motile and chemotactic, suggesting that chemotaxis has provided competitive advantage in contaminated soil environments [48]. *Pseudomonas putida* respond to chlorinated hydrocarbons that they perceive as potential carbon sources [49,31]. Chemotaxis to naphthalene has been observed in naphthalene-degrading species [42]. Deep subsurface bacteria have been shown to exhibit strong chemotactic responses to a variety of contaminants, including

trichloroethylene [32,39]. Researchers have suggested that chemotaxis is important in guiding subsurface microbial populations toward chemical contaminants [60,9,28]. A chemotactic response to an electron acceptor has been observed for *Pseudomonas stutzeri* KC, a natural aquifer isolate that transforms carbon tetrachloride under denitrifying conditions without the production of chloroform [17]. Dybas et al. reported migration of KC downstream of a conservative tracer in laboratory columns packed with aquifer material. They attributed this to a chemotactic response to nitrate gradients generated by metabolism [61]. After employing bioaugmentation to accelerate TCE degradation for a pilot study at Dover Air Force Base (Dover, DE) it was reported that bacteria injected into the center inoculation well were found in the outside

* Corresponding author.

E-mail address: rnf3f@virginia.edu (R.M. Ford).

Nomenclature

a	chemoattractant concentration [moles/L ³]	v_c	chemotactic velocity [L/T]
b	bacterial concentration [1/L ³]	$v_{c,pore}$	chemotactic velocity in a pore [L/T]
c	parameter characteristic of geologic media [L ^{1-m}]	x	distance [L]
d_{pore}	pore diameter [L]	α	turn angle between successive runs [deg]
D	diffusivity [L ² /T]	α_L	longitudinal dispersivity [L]
D_{eff}	effective diffusion coefficient in porous medium [L ² /T]	α_p	turn angle between successive runs restricted in a pore [deg]
D_K	Knudsen diffusion coefficient [L ² /T]	χ_0	chemotactic sensitivity coefficient [L ² /T]
E	dispersion coefficient [L ² /T]	λ	length of the run between tumbles [L]
K_d	chemotaxis receptor constant [moles/L ³]	μ	random motility coefficient [L ² /T]
L	longitudinal distance [L]	μ_{eff}	effective (or apparent) motility coefficient [L ² /T]
m	scaling exponent [-]	μ_K	random motility coefficient restricted in a pore [L ² /T]
N_b	flux of bacteria [1/L ² T]	μ_{pore}	random motility coefficient in a pore [L ² /T]
t	time [T]	μ_0	random motility coefficient in the absence of a chemical concentration gradient [L ² /T]
u	average linear fluid velocity [L/T]	τ	tortuosity parameter [-]
v	individual cell swimming speed [L/T]		

monitoring wells (about 20 ft on either side) that were intended to be negative controls [19]. Chemotaxis was suggested as a possible mechanism for the observed migration. Although the studies described above clearly implicate chemotaxis as a potentially important process in bioremediation, the complexity of field-scale studies has not allowed the magnitude of the chemotactic effect to be distinguished.

In this paper, a selection of laboratory-scale studies, from swimming behavior of individual cells to packed columns, that focus on transport via motility and chemotaxis is highlighted. It is organized in the following manner. Transport properties in bulk aqueous solution are analyzed first, then how these properties are altered by the presence of a granular (porous) medium, initially for stagnant systems and then for homogeneous steady flow. A summary of measured motility and chemotaxis properties is also included in tabular format.

2. Molecular basis of motility and chemotaxis

Bacteria are able to sense and respond to chemical gradients through receptor molecules embedded in the cell membrane. Although individual *Escherichia coli* bacteria sense temporal changes in the number of occupied receptors [41], they also respond to spatial gradients because they actively swim through them, thus exposing the receptors to a temporal variation in chemical concentration. This distinguishes bacteria from larger cells (e.g., flagellated protozoa) which are able to instantaneously sense spatial gradients along the length of their cell body. *E. coli* bacteria sense chemoattractants such as aspartate in their surroundings when molecules of aspartate bind to the methyl-accepting chemotaxis proteins *tar* that span

the cell membrane. These binding events external to the cell membrane trigger a conformational change of the *tar* proteins on the cytoplasmic side of the cell membrane that initiates an internal cascade of phosphorylation reactions. Phosphate is passed from intracellular signaling molecules *cheA* to *cheY* and the increase in phosphorylated *cheY* suppresses flagellar motor reversal associated with a tumble event. Less frequent tumbling results in greater run lengths in the direction of the chemoattractant source and biases the overall migration in a direction that is perceived to be favorable for survival. In the absence of a chemical concentration gradient, phosphorylation of *cheY* is not augmented and tumbling occurs at regular intervals, about once every second. The chemosensory pathway and its regulation are well documented [57].

3. Swimming properties

The trajectories of swimming bacteria like *E. coli* are described as a series of runs and tumbles. Bacteria are propelled through surrounding media by rotation of helically-shaped flagella. When rotary motors that turn the flagella rotate counterclockwise, the 6–8 flagella on *E. coli* tend to form a coordinated bundle behind the cell body and the cell swims smoothly forward. When one or more of the motors reverse direction, the bundle unravels and the cell tumbles chaotically, reorienting itself prior to the start of another run [59]. By this alternating series of runs and tumbles, bacteria trace out a 3D random walk somewhat analogous to diffusion of molecules in a gas. A mathematical relationship between the run-and-tumble swimming behavior of individual cells and the observed spreading or diffusion of a population of bacteria, described by the

random motility coefficient in the absence of any chemical gradients, μ_0 , was derived by Lovely and Dahlquist [40], i.e.,

$$\mu_0 = \frac{\lambda v}{3} \frac{1}{1 - \langle \cos \alpha \rangle} \quad (1)$$

where v is the individual cell swimming speed, λ is the length of the run between tumbles and α is the turn angle between successive runs. The $\cos \alpha$ is averaged for an individual over a series of changes in swimming direction. The swimming properties of individual cells are then averaged over a population to calculate μ_0 . Because the run lengths are affected by the presence of a chemical gradient, in theory, the values for the random motility coefficient μ and μ_0 may differ [21,53], but for the experimental systems described herein the differences are negligible. Therefore, if the swimming speed, frequency of tumbling and turn angle distribution are known, the random motility coefficient can be calculated from Eq. (1). This relationship was experimentally validated for *E. coli* [37,51]. Using a tracking microscope, all three parameters can be assessed from bacterial trajectories [24]. Videomicroscopy has also been used to obtain 2D trajectories of bacteria swimming in the plane of focus [30]. Usually, videomicroscopy of the cells is performed near a surface in order to obtain more cells that stay with-

in the field of view, but the turn angle distribution reflects only a 2D projection of the actual distribution.

Swimming properties (speeds, run times, and turn angles) for several species of bacteria are listed in Table 1. Cell swimming speeds of 25 $\mu\text{m/s}$ (or 2.2 m/day) are similar in magnitude to typical pore water velocities in groundwater aquifers. Note that *E. coli* have a bias toward angles less than 90° which gives a small persistence to their random walk. *Pseudomonas* species have a bimodal turn angle distribution with a bias toward angles near zero and 180° , which results in a mean turn angle of 90° . This is likely due to the arrangement of flagella, tufted at one end of the cell body for *Pseudomonas* sp. rather than being distributed peritrichously as *E. coli*. The tufted flagella of *P. putida* appear to produce more forward and backward swimming in contrast to the tumble and reorient behavior typical of *E. coli*. A comparison of trajectories obtained with the tracking microscope for *Pseudomonas fluorescens* and *E. coli* are shown in Fig. 1. The path traced by *P. fluorescens* has a jagged appearance with more turn angles near 0° and 180° than the trajectory for *E. coli*.

4. Transport properties

Keller and Segel [35] proposed a phenomenological model to account for motility and chemotaxis in the con-

Table 1
Swimming properties for individual bacteria

Bacteria	Mean swimming speed ($\mu\text{m/s}$)	Mean run time (s)	Mean turn angle (degrees)	Reference	μ_0 ($\times 10^6 \text{ cm}^2/\text{s}$) ^c
<i>E. coli</i> AW405	14.2	0.86	68	[7]	0.92
<i>E. coli</i> NR50	28.7 (± 5.7)	0.86 (± 1.18)	82 (± 35)	[23]	2.7
<i>E. coli</i> HCB1	22.8 (± 5.4)	1.24 (± 1.16)	70 (± 40)	[37]	3.3
<i>P. putida</i> PRS2000	44	2.0	90	[30] ^a ; [16] ^b	13

^a Measurement of mean run time and swimming speed from videomicroscopy in a 2D plane.

^b Measurement of turn angle distribution from tracking bacteria in 3D.

^c Calculated from Eq. (1).

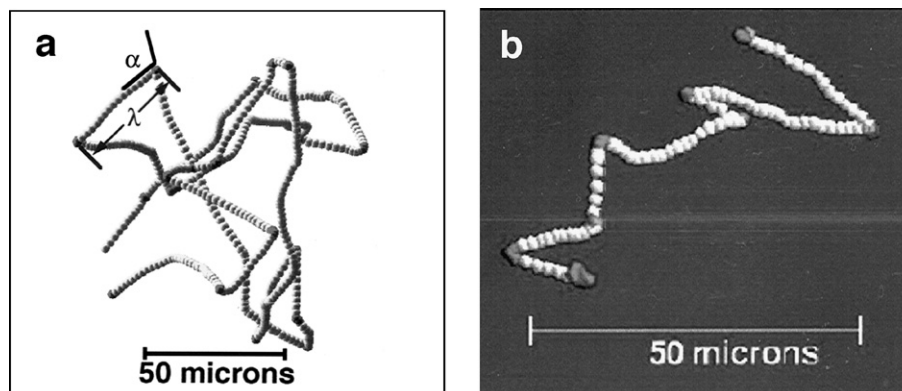


Fig. 1. Comparison of swimming trajectories obtained with the tracking microscope for (a) *E. coli* NR50 and (b) *P. fluorescens* PfO15. Spheres represent the location of the cell body at intervals of 1/12th of a second. Dark spheres indicate the position where a tumbling event occurred. The trajectory for PfO15 has more of a zig-zag appearance with more turn angles (defined by α) near 0° and 180° than the trajectory for *E. coli*.

text of a 1D flux expression with terms that are similar to diffusion and advection

$$N_b = -\mu \frac{db}{dx} + v_c b \quad (2)$$

The diffusive term in the expression for the flux of bacteria, N_b , is proportional to the gradient in bacterial concentration, b . The random motility coefficient, μ , is the proportionality constant which quantifies the diffusive behavior of a population of bacteria. The advective term in Eq. (2) is proportional to the bacterial concentration and quantifies the directed chemotactic response in terms of the chemotactic velocity, v_c . This expression is convenient because it is consistent with existing models for solute transport that are widely used in modeling field-scale transport. The driving force for the chemotactic velocity is a concentration gradient in a chemical stimulus or attractant rather than the hydraulic gradient associated with fluid velocity. For relatively shallow gradients which are typical in laboratory experiments and groundwater environments, the chemotactic velocity, v_c , is described by [13]

$$v_c = \frac{\chi_0}{3} \frac{K_d}{(K_d + a)^2} \frac{da}{dx} \quad (3)$$

The chemotaxis receptor constant, K_d , represents the propensity of the bacteria to bind the chemical attractant and, consequently, to sense gradients in chemoattractant concentration, a , in their surroundings. The K_d value in Eq. (3) is essentially an apparent binding constant that lumps together all the binding steps along the chemosensory pathway. Values for K_d are typically estimated from dose–response curves. For example, Mesibov et al. [44] report an effective K_d value of 0.125 mM for *E. coli* responding to α -methylaspartate. In some cases, the K_d value of the binding constant for the initial step in the chemosensory pathway is used. This assumes that this first step is also

the rate-controlling step in the process. Eisenbach [18] reports a K_d value of 0.5 μ M for the binding of aspartate to *tar* protein in *E. coli* and Hedblom and Adler [33] report a binding constant of 5 μ M for L-serine to Tsr. The chemotactic sensitivity coefficient, χ_0 , accounts for the mechanism by which bacteria respond to the gradient. The transport coefficients μ and χ_0 , which characterize the motility and chemotactic response of bacterial populations in bulk aqueous systems have been measured in well-controlled laboratory scale assays.

5. Motility and chemotaxis assays

Experimental assays to determine motility and chemotaxis parameters (essentially diffusion coefficients) were recently reviewed by Lewus and Ford [37]. For quantitative analysis, the capillary assay (along with its numerous variations) is the most widely used [1]. However, the stopped-flow diffusion chamber (SFDC) provides a better-controlled system for establishing well-defined initial conditions for subsequent mathematical analysis of experimental data [22,37]. Note that the range of values for the random motility coefficient reported in Table 2 is comparable to diffusion coefficients of small molecules such as sugars and amino acids to which the bacteria exhibit a chemotactic response. This is important because, if bacteria diffuse more slowly than the chemical to which they respond, the chemical gradient will dissipate before the bacteria are able to respond to it. If bacterial motility is much less than diffusion of the attractant chemical, then bacteria respond to out-dated information about their surroundings. In contrast to random motility coefficients of $2\text{--}19 \times 10^{-6} \text{ cm}^2/\text{s}$ observed for several species of bacteria, the Brownian diffusion coefficient for a non-motile colloid the same size as an *E. coli* bacterium is about three orders of magnitude smaller, i.e., $\sim 2.0 \times 10^{-9} \text{ cm}^2/\text{s}$ [6]. Thus, motility has a great impact

Table 2
Values of transport coefficients in bulk aqueous media

Bacteria	Random motility ($\times 10^6 \text{ cm}^2/\text{s}$)	Chemotactic sensitivity ($\times 10^4 \text{ cm}^2/\text{s}$)	Chemoattractant	Reference
<i>E. coli</i> NR-50	2.3 ^a			[20]
	2.3 ^b			[20]
	2.6 \pm 0.5			Unpublished data
<i>E. coli</i> HCB1		0.39 \pm 0.01	Fucose	[58]
		4.1 \pm 0.2	α -Methylaspartate	[58]
<i>E. coli</i> HCB1	2.9 \pm 1.4 ^a			[37]
	3.8 \pm 0.2 ^b			[37]
<i>P. putida</i> PRS2000		2.4	α -Methylaspartate	[37]
	35			[3]
<i>P. putida</i> G7		1.9 \pm 0.7	3-Chlorobenzoate	[3]
	0.32			[42]
		0.72	Naphthalene	[42]
		0.18 \pm 0.02,	Naphthalene	[50]
		2.9 \pm 1.1	Naphthalene	[50]

^a Calculated from swimming parameters measured with the tracking microscope using Eq. (1).

^b Measured in stopped-flow diffusion chamber (SFDC) experiments.

on the diffusion coefficient for a bacterium. Chemotactic sensitivity coefficients are two to three orders of magnitude greater than random motility coefficients for a given species. The response of *E. coli* to an amino acid analogue is about an order of magnitude greater than that for a sugar analogue.

6. Effective values for coefficients in porous media

The structure of porous media affects the swimming properties and transport coefficients of bacteria. Consider first the situation under static fluid conditions, i.e., without fluid flow. For transport in packed columns, an effective (or apparent) motility coefficient, μ_{eff} , is defined by [47]

$$\mu_{\text{eff}} = \frac{\mu_0}{\tau} \quad (4)$$

which introduces the tortuosity parameter, τ , for the presence of the porous medium. In theory, the tortuosity parameter accounts for the additional length of the diffusion path through a packed column that is required in order to move around the impenetrable solids. In practice, the tortuosity is essentially a fitting parameter that depends on characteristics of the porous medium and the interactions of the bacterium with the surface. Thus, laboratory measurements of tortuosity are not necessarily good predictors of field-scale transport.

Because bacteria have long run lengths relative to pore diameters typical of geologic media, their diffusivity is also reduced due to the limited size of the openings in the void space. A schematic drawing to represent bacterial trajectories within a porous medium is shown in Fig. 2. For situations in which average bacterial run lengths, λ , are larger than average pore diameters, d_{pore} , diffusion will be Knudsen-like and described according to [14]

$$D_K = \frac{d_{\text{pore}}v}{3} \quad (5)$$

In this case, the diffusion coefficient is defined by the diameter of the pores.

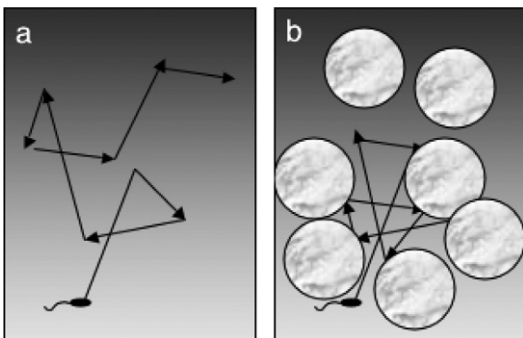


Fig. 2. Schematic representation of bacterial trajectories in a (a) bulk aqueous system and (b) porous medium of spherical grains. The presence of the impermeable spherical grains reduces the average run length and thereby also reduces the effective diffusion coefficient of bacteria in a packed column.

However, for situations in which the average pore size is comparable to the average bacterial run length, the random motility coefficient for a bacterium in granular media, μ_{pore} , is estimated using the harmonic average (a sum of resistances to mass transfer) prescribed by the Bosanquet equation [52]

$$\frac{1}{\mu_{\text{pore}}} = \frac{1}{\mu_0} + \frac{1}{D_K} \quad (6)$$

This relationship suggests that motility coefficients will be reduced in the presence of a porous medium, although the bacteria are still assumed to execute a random walk. Barton and Ford [4] and Chen et al. [12] showed that motility and chemotactic velocity were reduced by the same proportion due to collisions with pore walls according to

$$\frac{\mu_{\text{pore}}}{\mu_0} = \frac{v_{c,\text{pore}}}{v_c} = \left[1 + \frac{\lambda}{d_{\text{pore}}} \frac{1}{1 - \langle \cos \alpha \rangle} \right]^{-1} \quad (7)$$

For *E. coli* swimming in a porous medium (average pore diameter of 50 μm) at a speed of 25 $\mu\text{m/s}$ and a tumbling frequency of 1/s with a small persistence corresponding to an average turn angle of 70°, the transport parameters are reduced by about one-half.

Berg and Turner [8] observed in 10 μm -diameter capillaries that bacteria were unable to swim across the capillary and that their motion was restricted to moving primarily along the axis of the capillary. Chen et al. [12] formalized this observation in terms of a restricted turn angle distribution. The Bosanquet equation (6) assumes that the direction a bacterium swims following a collision with the surface is random and that all angles are possible. Therefore, in order to account for the turn angles being restricted in small diameter pores, we must modify the expression for Knudsen diffusion to reflect a biased turn-angle distribution, α_p ,

$$\mu_K = \frac{d_{\text{pore}}v}{3} \frac{1}{1 - \langle \cos \alpha_p \rangle} \quad (8)$$

Note that this equation is similar in form to the Lovely and Dahlquist expression in Eq. (1). If the turn angle distribution is restricted to smaller angles (less than 90°), then there is persistence to the random walk and the diffusion coefficient increases. Liu and Papadopoulos [38] showed that in small diameter capillaries (6 μm) *E. coli* were unable to turn around and reverse their direction. In this case, the bacteria are no longer able to carry out a diffusive process and their transport becomes wavelike.

The validity of the relationships in Eqs. (4)–(8) is difficult to test experimentally in a porous medium. This is because the opacity of the porous media precludes the use of a tracking microscope, the SFDC, and other motility assays that rely on light scattering. Alternative methods include capillary arrays at the population level, cellular dynamics computer simulations at the individual cell level, and magnetic resonance imaging (MRI) of packed columns at the population level. Effective transport coefficients from

these and other experiments in model porous media are tabulated in Table 3.

6.1. Capillary arrays

Berg and Turner [8] bundled capillary tubes together to create a porous medium with straight pores of uniform diameter. Thus, the theoretical tortuosity for this porous medium is unity. They measured the flux of bacteria from a reservoir on one side of the bundle to the other side. For 10 μm diameter capillaries, the motility coefficient was about twice that measured in 50 μm diameter tubes. Thus, the motility coefficient actually increased in the smaller capillary tubes. Berg and Turner referred to this phenomenon as capillary guidance. The aforementioned increases in apparent motility are consistent with predictions from the orientation model of Chen et al. [12] and suggest that directional persistence increases because bacteria are restricted to turning within a substantively restricted range of angles. Also, the chemotactic velocity toward aspartate was about two times larger in the 10 μm diameter capillaries than in the 50 μm ones. Corresponding chemotactic sensitivity coefficients were calculated and are included in Table 3. They are slightly higher than values reported in Table 2 for α -methylaspartate in the bulk.

6.2. Cellular dynamics simulations

Duffy et al. [15] simulated a porous medium as a random packing of spheres with uniform diameter. These investigators then performed Monte Carlo simulations using the swimming properties determined from tracking experiments in the bulk to simulate 10^5 bacterial trajectories through the random packing of spheres. Using the Einstein relationship

$$\langle x^2 \rangle = 6D_{\text{eff}}t \quad (9)$$

the diffusion coefficient, D_{eff} , in the simulated porous medium could be calculated from the mean squared displacement, $\langle x^2 \rangle$, of the trajectories over the time t of the simulation. Duffy et al. [15] performed simulations of *P. putida* trajectories through a random packing of spheres with uniform particle diameter. For particle diameters over the range from 100 to 700 μm , the effective motility coefficient varied by a factor of 10 from $4.6 \times 10^{-7} \text{ cm}^2/\text{s}$ to $4.6 \times 10^{-6} \text{ cm}^2/\text{s}$. The simulated motility coefficients were about 3–30 times lower than the bulk value and decreased dramatically as sphere diameters were decreased to $\sim 100 \mu\text{m}$.

6.3. Packed columns

Barton and Ford [3] sectioned columns packed with fine sand of fairly uniform diameter to determine bacterial distributions in a diffusion experiment. Effective motility coefficients were estimated from the decay of an initial step change in bacterial density within the column over a period of about 24 h. The effective motility coefficients decreased with decreasing average grain size of the sand. These observations were consistent with the idea that bacterial run lengths are shortened as the average pore diameter decreases with decreasing particle size. Sherwood et al. [55] used immunomagnetic-labeling and MRI imaging to visualize bacterial distributions within packed columns non-invasively. This technique not only provided better resolution, so experiments could be conducted over a shorter period of time, it also allowed a time series of bacterial density profiles to be collected within the same column. Using this technique, an effective diffusion coefficient for *E. coli* was evaluated and compared to a theoretical value calculated from Eq. (4); the bulk motility coefficient for *E. coli* was divided by a tortuosity determined independently using MnCl_2 as a tracer in the column. The experimentally observed motility was about

Table 3
Values of effective transport coefficients in porous media

Bacteria	Porous medium characteristics	Random motility ($\times 10^6 \text{ cm}^2/\text{s}$)	Chemotactic sensitivity ($\times 10^4 \text{ cm}^2/\text{s}$)	Attractant	Reference
<i>E. coli</i> AW405	Glass capillary array				[8]
	10 μm diameter pore	5.19 ± 1.01	13^{b}	L-aspartate	
	50 μm diameter pore	2.63 ± 0.42	5.7^{b}	L-aspartate	
Simulated <i>P. putida</i>	Spheres of uniform diameter (100–700 μm)	0.046–0.46			[15]
<i>E. coli</i> NR50	Glass-coated polystyrene (250 μm diameter)	0.50 ± 0.11			[55]
<i>P. putida</i> F1	Glass coated polystyrene (250 μm diameter)	$0.15 \pm 0.37^{\text{a}}$			[46]
			$0.08 \pm 0.01^{\text{a}}$	TCE	
<i>P. putida</i> PRS2000	Clean quartz sand				[3]
	81 μm diameter	0.7			
	137 μm diameter	0.48			
	194 μm diameter	1.6			
<i>P. putida</i> G7	326 μm diameter	3.1			
	Glass beads (50 μm diameter)		1.3	Naphthalene	[50]

^a Averaged value from two reported trials.

^b Estimated from reported drift velocities using Eq. (3).

3-fold less than the theoretical value, which suggested that the presence of the spherical packing significantly reduced the average bacterial run length. Average run lengths for *E. coli* are typically 25–30 μm compared with an approximate average pore diameter of 80 μm for a packed bed of 250 μm -diameter spheres. Olson et al. [46] have used the immunomagnetic-labeling and MRI imaging technique to evaluate chemotactic sensitivity coefficients in porous media for *P. putida* responding to trichloroethylene (TCE). Because run lengths for *P. putida* are 3–4 times longer than *E. coli*, the motility coefficient is reduced more severely in a packed column by as much as 85-fold less than the bulk value.

7. Dispersion coefficients

The focus to this point has been on motility and chemotaxis coefficients measured in static systems. In systems with fluid flow, how will motility and chemotaxis impact dispersion? Two factors contribute to dispersion – effective diffusion and mechanical mixing due to flow patterns along the porous network. These contributions to the dispersion coefficient E are represented in the following equation:

$$E = \frac{D}{\tau} + \alpha_L u \quad (10)$$

where α_L is the dispersivity in the direction of flow and u is the average linear fluid velocity. Because diffusion coefficients for motile bacteria are three orders of magnitude greater than for non-motile bacteria, the first term in Eq. (10) will be significantly increased due to motility. However, for velocities typical of ground water (1 m/day) in granular media, it is the second term in Eq. (10) that dominates the dispersion coefficient. Dispersivity values for non-motile bacteria in laboratory experiments with fairly homogeneous sand columns ranged from 0.014 to 0.22 cm [34]. A chemotactic response to a chemical gradient aligned with the direction of fluid flow will increase the apparent velocity of the bacterial population and thereby increase the dispersion coefficient. The maximum chemotactic velocity is bounded by the swimming speed of an individual bacterium; swimming speeds of 44 $\mu\text{m/s}$ reported for *P. putida* [30] are comparable to groundwater velocities of a meter per day ($\sim 10 \mu\text{m/s}$). Chemoattractant gradients that are not aligned with the fluid flow will divert bacteria from the flow direction and contribute to an increase in dispersivity. Thus, chemotaxis may provide a mechanism for increased dispersion and mixing of bacterial populations within saturated porous media.

Morley et al. [45] investigated dispersion of non-motile bacteria transverse to flow in laboratory columns. The columns were packed to create a vein of coarse-grain sand in the center surrounded by an annulus of fine-grain sand. Transverse mixing of bacteria across the coarse and fine layers was measurable and adequately characterized in terms of a transverse dispersion coefficient. Chemotaxis may provide a mechanism to enhance bacterial dispersion

across layers of granular media with different fluid permeabilities. For bioremediation applications, if a chemical pollutant is retained in a less permeable layer, a gradient in concentration may be created as the pollutant leaches out into the more permeable layer surrounding it and illicit a chemotactic response from bacteria.

To reduce the complexity of the porous medium, Lanning and Ford measured dispersion coefficients in well-defined 2D pore networks created by photolithography [36]. Because the pore networks were etched into glass plates, visualization of bacterial density profiles was possible using light-scattering. Dispersivity values in these micromodels were 0.28 cm for a cross-hatched network and 0.33 cm for staggered cylinders. It is surprising that dispersion is relatively high in these highly ordered systems, but not without precedent [27]. Lanning and Ford also reported that the contribution of bacterial motility to dispersion was negligible in their micromodel systems for $Pe > 5$.

8. Extension to the field scale

Prediction of transport for non-motile microorganisms being advected through granular aquifers has proven to be a much more complex matter than simple extrapolations of the governing parameters from the column to the field scale [29]. It is expected that the same will be true for motile bacteria. For bioaugmentation, the effect of bacterial motility and chemotaxis on longitudinal dispersivity α_L at the field scale may be a consideration. However, this would be difficult to predict from the aforementioned column-scale studies, in part, because of uncertainties relating to the scale-dependency of the measurements and to physical differences in the media. For conservative solutes being advected through unconsolidated aquifer sediments, the type of α_L scale-dependency described by Gelhar et al. [26] is now well documented. Using large sets of data compiled from many different studies, Schulze-Makuch [54] reported that for solutes being transport through unconsolidated sediments over distances between 10^{-1} and 10^5 m, α_L could be predicted fairly accurately by the following equation:

$$\alpha_L = cL^m \quad (11)$$

where c is a parameter characteristic of the geologic medium, L is the longitudinal distance, and m is the scaling exponent equivalent to the slope of the linear regression of the data plotted on a log–log plot of α_L vs L .

Not surprisingly, there is also a dependence of α_L upon travel distance for bacteria being advected through unconsolidated granular media. However, the nature of the relationship between longitudinal bacterial dispersion and the scale of the measurement is less clear because of the scarcity of applicable data, particularly at the field scale, and because of additional complexities, such as the demonstrated dependence of α_L on colloidal size [2]. Longitudinal dispersivities of <1 mm are typically reported for bacteria

being advected through sandy media in column-scale transport studies (e.g. [34]), whereas α_L estimates of several cm have been reported for small-scale (<10 m travel distance) field scale tests (e.g. [28]). The few quantitative assessments of bacterial transport on large scales >100 m indicate that α_L can be quite large. For example, Sinton et al. [56] report an α_L of 1.8 m for *E. coli* J6-2 being advected through ~400 m of an alluvial aquifer in New Zealand.

The potential significance of bacterial motility and (or) chemotaxis in the transport of bacteria in the direction of flow at the field scale is unclear and obtaining measurements for subsurface microbial transport properties in the field is expensive and technically challenging. Observations of motility and chemotaxis at the field-scale are mostly anecdotal. One notable exception is a recent study at the USGS toxics hydrology field site at Cape Cod, MA (Harvey and Metge, unpublished). They observed that a motile pseudomonad which was advected through sandy aquifer sediments under natural-gradient conditions arrived in down-gradient wells ahead of a non-motile mutant. Interestingly, in another injection and recovery study conducted in fractured granite at Mirror Lake, NH the same non-motile mutant exhibited greater fractional recovery at the downgradient well [5]. These Mirror Lake results are consistent with the idea that motile bacteria with higher diffusion coefficients would have more collisions with surfaces and would thereby be more readily filtered out. Motile bacteria may also be more likely to swim into stagnant pore water that would also increase their retention times in the fractured rock. Laboratory studies combined with additional field-scale work are needed to test these hypotheses.

For contaminated granular aquifers characterized by highly stratified deposits, low vertical dispersivities, and layers or lenses of fine material that can serve as reservoirs for release of dissolved organic contaminants into adjacent, more-conductive zones, a more relevant possibility for a chemotactic role might involve enhanced vertical migration of motile bacteria. The USGS groundwater toxics study site in Cape Cod, MA involves a good example of well-sorted/highly layered aquifer sediments that are contaminated with a variety of anthropogenic organic compounds. Results from a large (280 m) natural gradient tracer test performed in a three-dimensional sampling array instrumented with over 10,000 sampling ports indicate that although longitudinal dispersivity is generally quite large (0.96 m), the transverse vertical dispersivity is very small (1.5 mm) [25]. To estimate how important bacterial chemotaxis in the vertical direction may be relative to bacterial dispersion, a simple calculation is performed to compare the relative magnitude of chemotaxis and dispersion. To calculate a dispersion coefficient we multiply the dispersivity by the groundwater velocity (0.4 m/day at the site) to yield $0.7 \times 10^{-4} \text{ cm}^2/\text{s}$. Chemotactic sensitivity coefficients for *E. coli* responding to α -methylaspartate are in the range of 2.4×10^{-4} – $7.5 \times 10^{-4} \text{ cm}^2/\text{s}$ [34]. Thus, given the small, almost-negligible transverse vertical dispersivity that characterizes advective subsurface transport at the Cape Cod

site, a chemotactic response in the vertical direction at the field-scale may be significant. Further study is needed to begin to quantify the impact of chemotaxis on bacterial fate and transport at the field scale.

9. Conclusions

The value of laboratory scale measurements is the insight gained from the factors that relate individual cell swimming behavior to macroscopic-level population behavior. Laboratory scale experiments also allow for control over the properties of the porous medium characteristics to isolate the impact of features such as grain size. While relationships such as those in Eqs. (2) and (3) have been confirmed in laboratory scale experiments [37], in which bacteria respond over minutes or hours to 1D gradients over lengths scales of millimeters or centimeters, a remaining issue is to properly up-scale the equations to length and time scales appropriate for field studies. Before that can be accomplished the theoretical relationships for transport in granular media with flow must be validated and the effects of attachment and filtration included. The challenge remains to scale-up to the next level that involves much more complicated systems.

In laboratory studies designed to measure transport coefficients, operating conditions were selected to minimize complicating effects such as attachment and filtration, whereas in the field these are often significant factors. Thus, attachment and filtration may significantly alter the observed transport behavior between laboratory and field studies. Therefore, laboratory studies which examine both chemotaxis and attachment are necessary to advance the understanding of bacterial transport in groundwater systems. Although this important aspect was not addressed in this paper, the interested reader may consult several studies in the literature that measure and compare attachment rates for motile and non-motile bacteria [10,11,43].

Acknowledgement

R.M.F. gratefully acknowledges the contributions of many former students to this body of knowledge and support from the US Geological Survey and the University of Virginia Sesquicentennial Leave Program during the time this review was written.

References

- [1] Adler J, Dahl MM. A method for measuring the motility of bacteria and for comparing random and non-random motility. *J Gen Microbiol* 1967;46:161–73.
- [2] Auset M, Keller AA. Pore-scale processes that control dispersion of colloids in saturated porous media. *Water Resour Res* 2004;40:W03503. doi:10.1029/2003WR002800.
- [3] Barton JW, Ford RM. Determination of effective transport coefficients for bacterial migration in sand columns. *Appl Environ Microbiol* 1995;61:3329–35.
- [4] Barton JW, Ford RM. Mathematical model for characterization of bacterial migration through sand cores. *Biotechnol Bioeng* 1997;53:487–96.

- [5] Becker MW, Metge DW, Collins SA, Shapiro AM, Harvey RW. Bacterial transport experiments in fractured crystalline bedrock. *Ground Water* 2003;41:682–9.
- [6] Berg HC. *Random walks in biology*. Princeton (NJ): Princeton University Press; 1993.
- [7] Berg HC, Brown DA. Chemotaxis in *Escherichia coli* analysed by three-dimensional tracking. *Nature* 1972;239:500–4.
- [8] Berg HC, Turner L. Chemotaxis of bacteria in glass-capillary arrays. *Biophys J* 1990;58:919–30.
- [9] Bosma TNP, Schnoor JL, Schraa G, Zehnder AJB. Simulation model for biotransformation of xenobiotics and chemotaxis in soil columns. *J Contam Hydrol* 1988;2:225–36.
- [10] Camesano TA, Logan BE. Influence of fluid velocity and cell concentration on the transport of motile and non-motile bacteria in porous media. *Environ Sci* 1998;32:1699–708.
- [11] Camper AK, Hayes JT, Sturman PJ, Jones WL, Cunningham AB. Effects of motility and adsorption rate coefficient on transport of bacteria through saturated porous media. *Appl Environ Microbiol* 1993;59:3455–62.
- [12] Chen KC, Ford RM, Cummings PT. Mathematical models for motile bacterial transport in cylindrical tubes. *J Theor Biol* 1998;195:481–504.
- [13] Chen KC, Ford RM, Cummings PT. Perturbation expansion of Alt's cell balance equations reduces to Segel's 1D equations for shallow chemoattractant gradients. *SIAM J Appl Math* 1998;59:35–57.
- [14] Cussler EL. *Diffusion–mass transfer in fluid systems*. 2nd ed. New York: Cambridge University Press; 1997. p. 177.
- [15] Duffy KJ, Cummings PT, Ford RM. Random walk calculations for bacterial migration in porous media. *Biophys J* 1995;68:800–6.
- [16] Duffy KJ, Ford RM. Turn angle and run time distributions characterize swimming behavior for *Pseudomonas putida*. *J Bacteriol* 1997;179:1428–30.
- [17] Dybas MJ, Barcelona M, Bezborodnikov S, Davies S, Forney L, Heuer H, et al. Pilot evaluation of bioaugmentation for in-situ remediation of a carbon tetrachloride-contaminated aquifer. *Environ Sci Technol* 1998;32:3598–611.
- [18] Eisenbach M. Signal transduction in bacterial chemotaxis. In: Spudis JL, Satir BH, editors. *Sensory receptors and signal transduction*. New York: Wiley-Liss; 1991. p. 137–208.
- [19] Ellis DE, Lutz EJ, Buchanan RJ, Lee MD, Bartlett CL, Harkness M, et al. Bioaugmentation for accelerated in situ anaerobic bioremediation. Paper presented at In Situ and On-Site Bioremediation, The Fifth International Symposium, April 19–22, 1999, San Diego, CA; 1999.
- [20] Ford RM, Frymier PD, Lee J, Cummings PT. Presented at the American Institute of Chemical Engineers Annual Meeting, San Francisco, CA; 1994.
- [21] Ford RM, Lauffenburger DA. Analysis of chemotactic bacterial distributions in population migration assays using a mathematical model applicable to steep or shallow attractant gradients. *Bull Math Biol* 1991;53:721–49.
- [22] Ford RM, Phillips BR, Quinn JA, Lauffenburger DA. Measurement of bacterial random motility and chemotaxis coefficients. I. Stopped-flow diffusion chamber assay. *Biotechnol Bioeng* 1991;37:647–60.
- [23] Frymier PD, Ford RM. Analysis of bacterial swimming speed approaching a solid–liquid interface. *AIChE J* 1997;43:1341–7.
- [24] Frymier PD, Ford RM, Berg HC, Cummings PT. Three-dimensional tracking of motile bacteria near a solid planar surface. *Proc Natl Acad Sci USA* 1995;92:6195–9.
- [25] Garabedian SP, Leblanc DR, Gelhar LW, Celia MA. Large-scale natural gradient tracer test in sand and gravel, Cape Cod, Massachusetts. 2. Analysis of spatial moments for a nonreactive tracer. *Water Resour Res* 1991;27:911–24.
- [26] Gelhar LW, Welty C, Rehfeldt KR. A critical review of data on field-scale dispersion in aquifers. *Water Resour Res* 1992;28:1955–74.
- [27] Gunn D, Pryce C. Dispersion in packed beds. *Trans Inst Chem Eng* 1969;47:T341–50.
- [28] Harvey RW, Garabedian SP. Use of colloid filtration theory in modeling movement of bacteria through a contaminated sandy aquifer. *Environ Sci Technol* 1991;25:178–85.
- [29] Harvey RW, Harms H. Transport of microorganisms in the terrestrial subsurface: in situ and laboratory methods. In: Hurst CJ, Knudsen GR, McInerney MJ, Stetzenback LD, Crawfordd RI, editors. *Manual of environmental microbiology*. 2nd ed. Washington: AMS Press; 2001. p. 753–76.
- [30] Harwood CS, Fosnaugh K, Dispensa M. Flagellation of *Pseudomonas putida* and analysis of its motile behavior. *J Bacteriol* 1989;171:4063–6.
- [31] Harwood CS, Parales RE, Dispensa M. Chemotaxis of *Pseudomonas putida* toward chlorinated benzoates. *Appl Environ Microbiol* 1990;56:1501–3.
- [32] Hazen TC. Deep subsurface bacteria responses to contaminants. In: *Proceedings of the first international symposium on microbiology of the deep subsurface*, Aiken, SC, WSRC Information Services; 1989.
- [33] Hedblom ML, Adler J. Genetic and biochemical properties of *Escherichia coli* mutants with defects in serine chemotaxis. *J Bacteriol* 1980;144:1048–60.
- [34] Hornberger GM, Mills AL, Herman JS. Bacterial transport in porous media: evaluation of a model using laboratory observations. *Water Resour Res* 1992;28:915–38.
- [35] Keller EF, Segel LA. Model for chemotaxis. *J Theor Biol* 1971;30:225–34.
- [36] Lanning LM, Ford RM. Glass micromodel study of bacterial dispersion in spatially periodic porous networks. *Biotechnol Bioeng* 2002;78:556–66.
- [37] Lewus P, Ford RM. Quantification of random motility and chemotaxis bacterial transport coefficients using individual-cell and population-scale assays. *Biotechnol Bioeng* 2001;75:292–304.
- [38] Liu Z, Papadopoulos KD. Unidirectional motility of *Escherichia coli* in restrictive capillaries. *Appl Environ Microbiol* 1995;61:3567–72.
- [39] Lopez de Victoria G. Chemotactic behavior of deep subsurface bacteria toward carbohydrates, amino acids and a chlorinated alkene. MS thesis, University of Puerto Rico, Río Piedras; 1989.
- [40] Lovely PS, Dalquist FW. Statistical measures of bacterial motility and chemotaxis. *J Theor Biol* 1975;50:477.
- [41] Macnab RM, Koshland DE. The gradient-sensing mechanism in bacterial chemotaxis. *Proc Natl Acad Sci USA* 1972;69:2509–12.
- [42] Marx RB, Aitken MD. Quantification of chemotaxis to Naphthalene by *Pseudomonas putida* G7. *Appl Environ Microbiol* 1999;65:2847–52.
- [43] McClaine JW, Ford RM. Characterizing the adhesion of motile and nonmotile *Escherichia coli* to a glass surface using a parallel plateflow chamber. *Biotechnol Bioeng* 2002;78:179–89.
- [44] Mesibov R, Ordal G, Adler J. The range of attractant concentrations for bacterial chemotaxis and the threshold and size of response over this range. *J Gen Physiol* 1973;23:203.
- [45] Morley LM, Hornberger GM, Mills AL, Herman JS. Effects of transverse mixing on heterogeneous porous media. *Water Resour Res* 1998;34:1901–8.
- [46] Olson MS, Ford RM, Smith JA, Fernandez EJ. Quantification of bacterial chemotaxis in porous media using magnetic resonance imaging. *Environ Sci Technol* 2004;38:3864–70.
- [47] Olson MS, Smith JA, Ford RM, Fernandez EJ. Analysis of column tortuosity for MnCl₂ and bacterial diffusion using magnetic resonance imaging (MRI). *Environ Sci Technol* 2005;39:149–54.
- [48] Pandy G, Jain RK. Bacterial chemotaxis toward environmental pollutants: role in bioremediation. *Appl Environ Microbiol* 2002;68(12):5789–95.
- [49] Parales RE, Ditty JL, Harwood CS. Toluene-degrading bacteria are chemotactic towards the environmental pollutants benzene, toluene, and trichloroethylene. *Appl Environ Microbiol* 2000;66(9):4098–101.
- [50] Pedit JA, Marx RB, Miller CT, Aitken MD. Quantitative analysis of experiments on bacterial chemotaxis to naphthalene. *Biotechnol Bioeng* 2002;78:626–34.

- [51] Phillips BR, Quinn JA. Random motility of swimming bacteria: single cells compared to cell populations. *AIChE J* 1994;40:334–48.
- [52] Pollard WG, Present RD. On gaseous self-diffusion in long capillary tubes. *Phys Rev* 1948;73:762–74.
- [53] Rivero MA, Tranquillo RT, Buettner HM, Lauffenburger DA. Transport models for chemotactic cell populations based on individual cell behavior. *Chem Eng Sci* 1989;44:2881–97.
- [54] Schulze-Makuch D. Longitudinal dispersivity data and implications for scaling behavior. *Ground Water* 2005;43:443–56.
- [55] Sherwood JL, Sung JC, Ford RM, Fernandez EJ, Maneval JE, Smith JA. Analysis of bacterial random motility in a porous medium using magnetic resonance imaging and immunomagnetic labeling. *Environ Sci Technol* 2003;37:781–5.
- [56] Sinton LW, Finlay RK, Pang L, Scott DM. Transport of bacteria and bacteriophages in irrigated effluent into and through an alluvial gravel aquifer. *Water, Air, Soil Pollut* 1997;98:17–42.
- [57] Stock JM, Surette MG. Chemotaxis. In: Neidhardt FC, editor. *Escherichia coli* and *Salmonella*: cellular and molecular biology. 2nd ed. Washington, DC: American Society of Microbiology; 1996. p. 1103–29.
- [58] Strauss I, Frymier PD, Hahn CM, Ford RM. Analysis of bacterial migration. II. Studies of multiple attractant gradients. *AIChE J* 1995;41:402–14.
- [59] Turner L, Ryu WS, Berg HC. Real-time imaging of fluorescent flagellar filaments. *J Bacteriol* 2000;182:2793–801.
- [60] van der Meer JR, Roelofsen W, Schraa G, Zehnder A JB. Degradation of low concentrations of dichlorobenzenes and 1,2,4-trichlorobenzene by *Pseudomonas* sp. strain P51 in nonsterile soil columns. *FEMS Microbiol Ecol* 1987;45:333–41.
- [61] Witt ME. Michigan State University, East Lansing, MI, personal communication.